ROTORDYNAMIC DEVELOPMENTS FOR HIGH SPEED MULTISTAGE PUMPS

by

Stanley E. Pace

Project Engineer

Steam Turbines and Related Auxiliaries

Electric Power Research Institute

Palo Alto, California

Stefan Florjancic

Development Engineer

Pump Division

and

Ulrich Bolleter

Head, Laboratory for Vibrations and Acoustics

Sulzer Brothers, Limited

Winterthur, Switzerland

Stanley E. Pace is a Project Manager in the Availability and Life Extension Program, Coal Combustion Systems Division, at the Electric Power Research Institute (EPRI) in Palo Alto, California. He is responsible for managing research and development projects involving steam turbines, pumps and related auxiliaries.

Prior to joining the Institute in 1984, Mr. Pace was Manager of Mechanical Engineering at United Centrifugal Pump, San Jose, California, and Section Manager of Nuclear Pump Engineeering at CE-KSB, Newington, New Hampshire. He received a B.S. degree in Mechanical Engineering (1967) and an M.S. degree in Mechanical Engineering (1969) from Lehigh University. Mr. Pace is a member of ASME.

Stefan Florjancic graduated in 1982 from the Federal Institute of Technology in Zurich, Switzerland, with a degree in Mechanical Engineering. After training periods in pump factories in West Germany, U.S.A., France and Brazil during his studies, he joined Sulzer Brothers Limited, Switzerland in 1983, and is now working in the area of mechanical development and design of pumps. His major tasks have been rotordynamic calculations and research on rotordynamic coefficients of labyrinth seals.

Ulrich Bolleter graduated in 1966 from Winterthur Technical College, Switzerland, with a degree in Electrical Engineering. He holds an M.S. degree in Mechanical Engineering from Arizona State University, and a Ph.D. degree in Engineering from Purdue University.

After a year of teaching vibrations and acoustics courses at Purdue University, he joined the Laboratory for Vibrations and Acoustics at Sulzer, and has been its Head since 1978.

Dr. Bolleter is engaged in experimental and theoretical research and development with many of Sulzer's products. He has published a number of papers in the areas of acoustics, blade vibrations, modal analysis, shell vibrations, weaving machines and pumps. Towards the end of 1984, he joined the Pump Division of Sulzer Brothers, Limited, as Technical Manager for special pumps, responsible for development and design.

ABSTRACT

At present, the major factor limiting the designer's ability to predict the rotordynamic behavior of multistage centrifugal pumps is the availability of accurate input data for the forces acting on the rotor. Recent results are presented from an ongoing research project sponsored by the Electric Power Research Institute at Sulzer Brothers on the measurement of hydraulic forces on impellers of high energy pumps. The best available coefficients for seals and impeller forces, derived from the research, are applied to a typical four stage diffuser style pump. The application of swirl breaks to impellers is demonstrated. The results of the analysis is then compared to actual test data. The conclusions highlight the importance of including impeller hydraulic forces in the rotordynamic analysis, the potential of swirl breaks to significantly improve rotor stability and areas needing further research.

INTRODUCTION

The task of correctly predicting the rotordynamic behavior of turbomachinery has challenged designers since they first encountered vibration related failures. As machine speeds and power concentrations increased, it became evident that the long term reliability of rotating equipment was closely related to rotordynamic behavior. Instead of the critical speed, which has often been considered the main criterion, stable, well damped rotordynamic response is now recognized as a necessary condition for high reliability [1, 2, 3]. The challenge the designers face is to accurately predict rotordynamic performance so that rotor behavior can be optimized within the constraints of the total machine performance during the design stage, rather than during shop tests or in the field, where the cost of changes will be high and the final result often less than optimum.

To accurately predict rotordynamic behavior, the designer needs not only the mathematical tools to model the rotor-bearing system, but also correct input data to enter into the model. The progress made in providing the designer with high quality mathematical tools has been excellent. Transfer matrix and finite element techniques are now readily available to the designer. At present, the major factor limiting the designer's ability to predict the rotordynamic behavior of multi-stage centrifugal pumps is the uncertainty in what to use for the forces acting on the rotor.

In multi-stage centrifugal pumps, the forces on the rotor arise from journal bearings, interstage seals (labyrinths), thrust balancing devices and hydraulic interaction between the impeller and the casing. The journal bearing forces can be approximated by linearized stiffness and damping coefficients when shaft motion does not exceed a third of the bearing clearance. Coefficients are well known from the theoretical and experimental work of individuals such as Orcutt, Schaffrath, Glienicke, Lund and Thompson [4, 5, 6, 7]. The forces at the interstage seals and balancing devices require stiffness, damping and mass coefficients to be adequately described in a linear system. For short plain seals, these coefficients can be approximated from the investigations of Black and Childs [8, 9, 10, 11]. However, for long seals, such as balance pistons, and seals with serrations or other complex geometry, adequate prediction methods do not exist. In the area of hydraulic forces between impeller and casing, several experimental investigations have been carried out [12, 13, 14, 15, 16]. However, little is known about the influence of geometrical parameters on the hydraulic forces produced by the impeller-casing interaction.

Hydraulic forces acting on the rotor can be classified into two categories:

- Forces which are present for a non-vibrating rotor (excitation forces).
- Forces which are created by lateral rotor vibration (hydrodynamic interaction forces).

The importance of both categories of forces has been recognized for some time. Recent results from an ongoing research project sponsored by the Electric Power Research Institute (EPRI) at Sulzer Brothers (Switzerland) on the measurement of hydraulic forces of impellers, will be applied to a high energy multistage pump, typical of boiler feed and water injection applications. The effects of the seals will be included based on calculations using the theory of Childs [11]. The objectives of this analysis are to:

- Provide a better understanding of the importance of impeller forces on rotor dynamic behavior.
- Demonstrate how, with better insight into the nature of the forces acting on the rotor, design changes can be developed which substantially improve rotor stability.

The results of the analysis of a four-stage pump will be presented to illustrate the influence of seals, impellers and balance pistons on the predicted rotordynamic behavior. The application of swirl breaks within a pump stage will be presented and the effects of swirl breaks on rotor stability will be discussed. The results of the rotordynamic analysis will be compared to actual test vibration, taken from the pump analyzed, while operating near the stability limit. The areas of uncertainty in the data and future research needs will be presented.

PUMP

The pump used in the analysis is a horizontal, four-stage, diffuser style pump with a balance piston to control axial thrust (Figure 1). The hydraulic performance data at the best efficiency point (BEP) and the recommended minimum flow, as well as some geometrical data, is given in Table 1. The rotor is supported by two, four lobe, oil lubricated journal bearings, and the residual axial thrust is taken by a double acting, tilting pad thrust

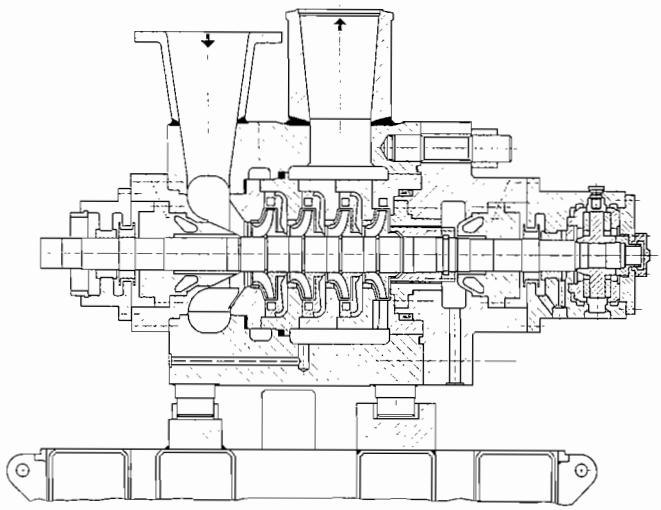

Figure 1. Cross Section of Typical Boiler Feed Pump.

Table 1: Main Data of Pump.

Hydraulic Data	BEP (Qoo)	Min. flow (QLo)
Q (m^3/s)	0.335	0.082
(Gpm)	5310	1300
n (cpm)	6200	6200
H_{tot} (m)	2195	2582
(ft)	7201	8471
H_{stage} (m)	549	646
(ft)	1801	2119
Degree of (–) reaction	0.74	0.76
T (°C)	149	149
(°F)	300	300

Geometrical Data		
Overall length of rotor:	2.21 m	(7.25 ft)
Distance between centerlines of bearings:	1.675 m	(5.50 ft)
Distance between stages:	0.141 m	(0.46 ft)
Assembled rotor weight:	444 kg	(979 lb)
Impeller weight: (including 1ℓ (0.26 gal) of water):	16 kg	(35 lb)
Unbalance mass applied at coupling:	3.75×10^{-3}kg·m	(27.1×10^{-3}lb·ft)

bearing. Bearing load is normally established by assigning approximately half of the rotor weight to each bearing. However, the measurement of static radial thrust in the test machine showed that radial thrust produced by a suction impeller due to inlet asymmetry can be on the order of half the total rotor weight. The direction of this force depends on the flow, manufacturing tolerances and the orientation of suction piping. Therefore, one case was calculated using only 20 percent of the total rotor weight on the bearings to account for the possible effect of radial thrust.

All internal seals, including the piston, have small shallow serrations machined into the stationary parts. The suction seal (neck ring) at the first stage is a straight seal, the other three seals are stepped. The balance piston is broken divided into four sections by three deep grooves in the stationary part. The pump is equipped with mechanical shaft seals and driven through a gear type coupling.

MODEL

The rotor was modelled using the MADYN computer program [17]. The MADYN program is a finite element based program which will accept non-symmetric stiffness and damping matrices, gyroscopic forces, harmonic and transient excitation. Forces acting on the rotor are described as follows:

$$-\begin{bmatrix}F_1\\F_2\end{bmatrix}=\begin{bmatrix}K_{11} & k_{12}\\k_{21} & K_{22}\end{bmatrix}\cdot\begin{bmatrix}X_1\\X_2\end{bmatrix}+\begin{bmatrix}C_{11} & c_{12}\\c_{21} & C_{22}\end{bmatrix}\cdot\begin{bmatrix}\dot{X}_1\\\dot{X}_2\end{bmatrix}+\begin{bmatrix}M_{11} & m_{12}\\m_{21} & M_{22}\end{bmatrix}\cdot\begin{bmatrix}\ddot{X}_1\\\ddot{X}_2\end{bmatrix} \quad (1)$$

Based on the rotational symmetry of the seals and impellers the following assumptions of isotropy were made:

$$K_{11}=K_{22} \qquad C_{11}=C_{22} \qquad M_{11}=M_{22}$$
$$-k_{12}=k_{21} \qquad -c_{12}=c_{21} \qquad -m_{12}=m_{21}$$

Undamped natural frequencies with gyroscopic effects, damped natural frequencies and forced rotor response can be calculated. The rotor model consisted of 51 stations with seven additional distributed masses representing the impellers, thrust collar, balancing piston and coupling. The polar and transverse moments of inertia of the impellers, thrust collar and coupling were included. Half the coupling spacer mass was added to the mass of the pump half coupling hub. No credit was taken for the stiffening effect of the shrink fits for the impellers and sleeves. The pump casing, foundation and bearing housing were considered to be infinitely stiff, compared to the rotor.

INPUT DATA

Selected geometrical data for journal bearings, seals and impellers are given in Table 2.

The coefficients for the seals and balance pistons were calculated with a computer program based on Childs' "finite length" theory [11]. The tangential velocity of the leakage flow along the impeller shroud was calculated by an integration with finite differences as a function of diameter, taking the different roughnesses of the rotating and stationary parts into account. The exit tangential velocity at the impeller outlet was used as the initial value. The pressure was reduced according to the rotation to yield the pressure difference across the seal [18]. For the stepped seals and the balance piston, the exit tangential velocity of one section was used as the initial tangential velocity for the next section. The pressure difference was split up according to diameters and the section lengths.

Table 2. Journal Bearing, Seals, Impeller Geometrical Data (new).

	Diameter (mm) (in)	Length (mm) (in)	Radial Clearance (mm) (in)	Remarks
Bearing	120 4¾	60 2⅜	0.084 0.0033	1.4 o/oo
First stage suction seal	230 9	25 1	0.45 0.018	straight
Normal stage suction	230/215 9/8½	12/12 ½ ½	0.45 0.018	stepped
Inter-stage bushing	165 6½	23 ⅞	0.43 0.017	straight
Piston	215 8½	180 7⅛*)	0.45 0.018	*) divided by grooves
Impeller	333 13⅛	26.4 *) 1	– –	*) impeller width at outlet

Inlet swirl brakes were introduced as radial slots in the surface of the casing opposite the impeller suction shroud, extending from the suction seal diameter to 56 percent of impeller outlet diameter (Figure 2). The purpose of the swirl break is to control

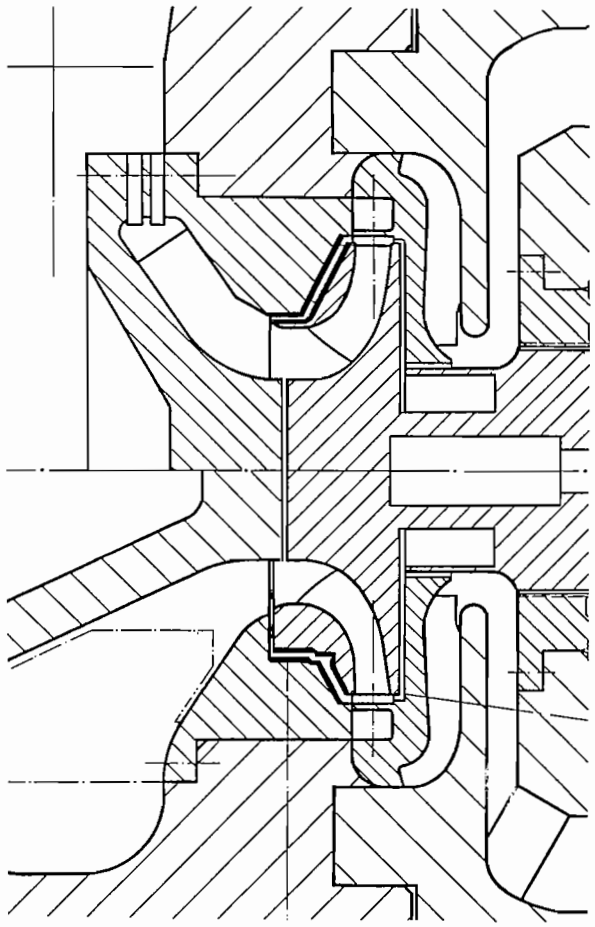

Figure 2. Swirl Breaks.

the co-rotational component of the fluid velocity in the space between the impeller and the casing, and entering the suction seal. Swirl breaks have been shown to be very effective in controlling instability problems originating in the balance piston [19]. For the cases with the swirl brakes, the calculated tangential velocity at the inlet to the suction seal and balance pistons is divided by two. The inlet swirl for interstage bushing is assumed to be zero for all cases.

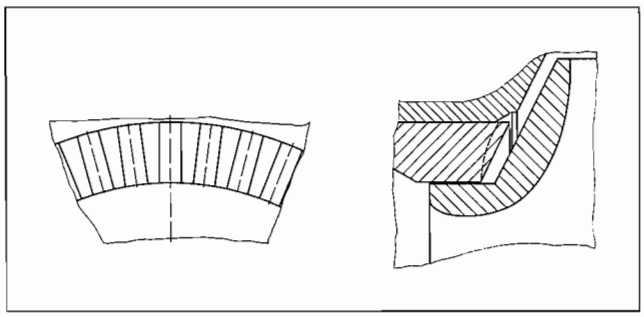

Figure 3. Partial Cross Section of Test Machine.

Stiffness and damping coefficients for the journal bearings are based on dimensionless experimental data provided by the bearing manufacturer.

The data for the impeller hydraulic forces was derived from testing described in [16]. Two configurations were used to determine impeller coefficients (shroud plus impeller hydraulics forces). Both configurations are shown in Figure 3. The difference between the two configurations can be summarized as follows:

- The impeller design is a standard configuration with an axial flow suction seal. Forces resulting from the seal were calculated theoretically and subtracted from the total measured forces to give coefficients for the impeller.
- The impeller design has been modified to incorporate a radial flow seal which produces negligible radial and tangential forces. The impeller forces alone are measured.

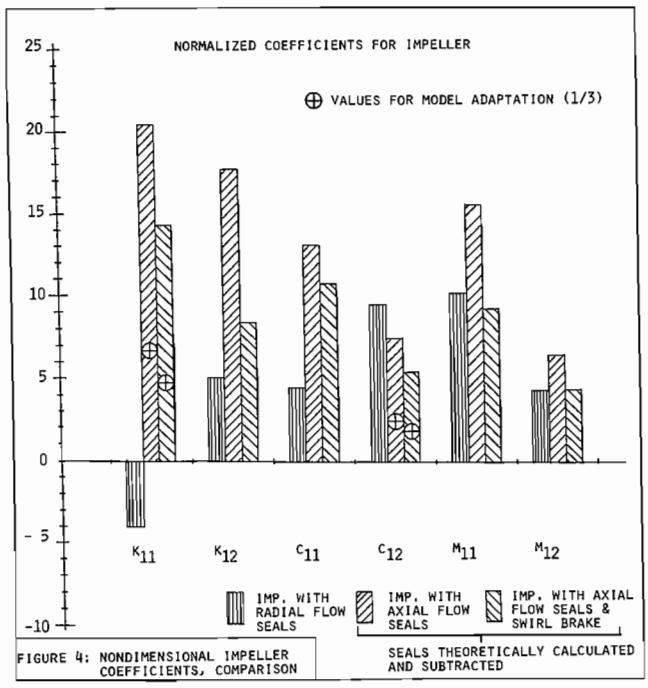

Figure 4. Nondimensional Impeller Coefficients, Comparison.

Results for tests with both configurations are presented in Figure 4 using the normalized form of Ohashi [21].

$$K_{11}^*, k_{12}^* = \frac{K_{11}, k_{12}}{\rho \cdot \pi/4 \cdot D_2^2 \cdot B_2 \cdot \omega^2} \quad (2)$$

$$C_{11}^*, c_{12}^* = \frac{C_{11}, c_{12}}{\rho \cdot \pi/4 \cdot D_2^2 \cdot B_2 \cdot \omega} \quad (3)$$

$$M_{11}^*, m_{12}^* = \frac{M_{11}, m_{12}}{\rho \cdot \pi/4 \cdot D_2^2 \cdot B_2} \quad (4)$$

A large discrepancy is noted between the two different methods, 1 and 2. This effect is primarily attributed to the significant difference in shroud geometry necessary to accomodate the radial flow seal although the accuracy of the calculated seal coefficients may also have contributed to the difference. The additional axial gap for configuration 2 also produces additional, unwanted forces [22]. Configuration 1 with no geometrical changes intuitively appears to be more reliable and was used for the investigation.

Measured data were extrapolated from test conditions to pump design conditions with Equations (2), (3), and (4). This extrapolation assumes that these equations are representative similiarity relationships. This is an assumption which is not in total agreement with available data [16], but does provide a starting point for the analysis. A comparison of the measured natural frequency (least damped mode), which is at approximately 73 percent of the running speed for worn seals, with the corresponding calculated frequency suggested that further correction was necessary. The computed eigenfrequencies were too high; to bring the analysis more into agreement with the experimental measurements, the values of K_{11} and C_{12} were divided by three. This was the only adaptation of the data to the model. Clearly further tests at higher speeds and temperatures are needed for both impeller and seal forces.

The large influence of a swirl break, not only on the seal, but also on the impeller coefficients, is evident in Figure 4. K_{12}, the coefficient primarily responsible for the forward driving portion of the tangential force [16], was reduced to approximately 50 percent, resulting in a much more stable system. For the cases using the swirl breaks, the resulting K_{11} and C_{12} for the impellers were divided by three as discussed above.

Coefficients for seals, impellers and bearings are given in Table 3. The cross-coupled masses shown in the table can not be introduced directly into the computer code MADYN. Therefore, the cross-coupled stiffness was modified:

$$K_{12}' = K_{12} - m_{12}(\omega^2) \quad (5)$$

It should be noted that this is correct only for synchronous excitation. However, in the range of interest, approximately 0.5ω to 1.57ω, the error is negligible.

RESULTS OF CALCULATIONS

An overview of all eight cases calculated is given in Table 4. Case 4 will be discussed in detail first.

All the coefficients were calculated for a number of speeds: 3000 cpm, 4000 cpm, 5000 cpm, 6200 cpm and 7500 cpm. With each set of data eigenvalues, i.e., natural frequencies and damping, were calculated. Damping, D, is defined as

$$D = \frac{-Re(\lambda)}{[(Re(\lambda))^2 + (Im(\lambda)^2)]^{0.5}} \quad (6)$$

where
D>0 = damping
D<0 = exciting

The influence of the running speed on the damping and the natural frequency for six different mode shapes labeled "A" through "F" is shown in Figure 5. In this diagram the frequency axis (D=0) is the limit of stability. For Case 4, a typical mode shape for the mode labeled "A," which is tending toward instability at approximately 7100 cpm, is shown in Figure 6.

Table 3. Stiffness, Damping and Mass for Seals, Impeller and Bearings at Operating Speed.

			Stiffness (N/m)		Damping (Ns/m)		Mass (kg)	
seal	flow	clear-ance	K11	k12	C11	c12	M11	m12
First stage suction seal	Qoo	new	6.39×10^6	5.19×10^6	9.14×10^3	6.77×10^2	0.827	0.015
		worn	2.37×10^6	3.29×10^6	5.27×10^3	2.14×10^2	0.237	0.0004
	QLO	worn	4.01×10^6	1.18×10^6	7.38×10^3	1.07×10^2	0.220	−0.080
	Qoo	new	3.10×10^6	-2.86×10^4	5.08×10^3	1.71×10^2	0.486	−0.056
Interstage		worn	1.15×10^6	-1.06×10^4	2.98×10^3	5.88×10^1	0.159	−0.077
bushing	QLo	worn	1.41×10^6	-9.93×10^3	3.35×10^3	5.55×10^1	0.150	−0.073
Normal stage	Qoo	new	2.68×10^6	1.68×10^6	3.35×10^3	9.10×10^1	0.115	−0.006
suction seal		worn	8.07×10^5	1.09×10^6	1.89×10^3	7.69×10^0	0.013	−0.004
	QLo	worn	1.24×10^6	4.41×10^5	2.60×10^3	6.41×10^0	0.007	−0.020
Balance	Qoo	new	6.41×10^7	4.30×10^7	1.07×10^4	9.26×10^3	13.893	0.156
piston		worn	2.81×10^7	3.00×10^7	6.12×10^4	3.97×10^3	5.191	−0.107
	QLo	worn	3.62×10^7	1.56×10^7	7.07×10^4	2.709×10^3	5.227	−0.663

Impeller-Hydraulic-Interaction, including shroud forces

	flow	K11	k12	C11	c12	M11	m12
	Qoo	6.13×10^6	1.60×10^7	1.82×10^4	3.50×10^3	33.49	13.99
	Q10	4.40×10^6	2.39×10^7	3.15×10^4	4.67×10^3	33.92	17.60

Bearings

% rotor-weight on b	K11	k12	k21	K22	C11	c12	c21	C22
100%	3.82×10^7	2.41×10^7	-1.70×10^7	1.00×10^8	6.25×10^4	8.15×10^3	-4.30×10^3	1.20×10^5
20%	2.79×10^7	1.31×10^7	-1.31×10^7	2.95×10^7	5.10×10^4	2.12×10^3	-3.66×10^3	5.15×10^4

Table 4. Parameter Variation With Least Damped Eigenfrequencies and Damping.

						least damped mode	
Case	Labyrinths	Impeller Forces	Flow	Bearing Load	Swirl Break	Natural Frequency Hz	Damping D %
1	new	no	Qoo	weight	no	106	19
2	new	yes	Qoo	weight	no	93	13
3	worn	no	Qoo	weight	no	81	7
4	worn	yes	Qoo	weight	no	80	2
5	worn	yes	Qoo	0.2× weight	no	75	3
6	worn	yes	QLo	weight	no	90	13
7	worn	yes	Qoo	weight	yes	76	24
8	worn	yes	QLo	weight	yes	72	26

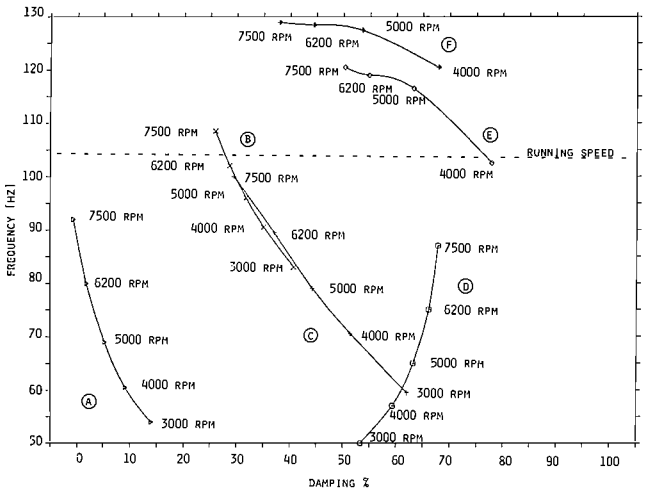

Figure 5. Eigenfrequency Versus Damping.

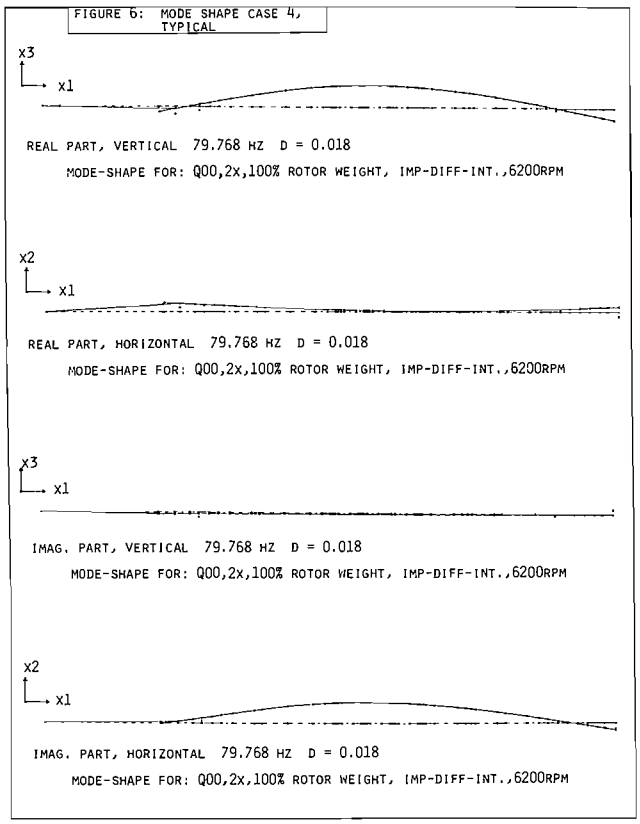

Figure 6. Mode Shape Case 4, Typical.

By definition, a "critical speed" occurs where the running frequency coincides with an eigenfrequency. This situation can be clearly seen in a Campbell diagram. A Campbell diagram for Case 4 is depicted in Figure 7. In accelerating up to running frequency, four 'critical speeds" are encountered. It should be noted that mode shape "D" is omitted from Figure 7, because it is a backward whirling mode and cannot be excited by imbalance. As the diagram indicates, even the least damped "critical speed" of mode shape "A" still has a damping of about 12 percent. More important is the fact that when the pump is at the normal running speed, this mode shape has an eigenfrequency of 0.77 × (running speed) and only two percent damping. This mode becomes unstable, as shown in Figure 5, at a pump speed of about 7100 cpm with an eigenfrequency around 88 Hz. Instabilities at a ratio of eigenfrequency to running speed of 0.75, with increased clearances (worn clearances), is not uncommon for high energy multistage pumps.

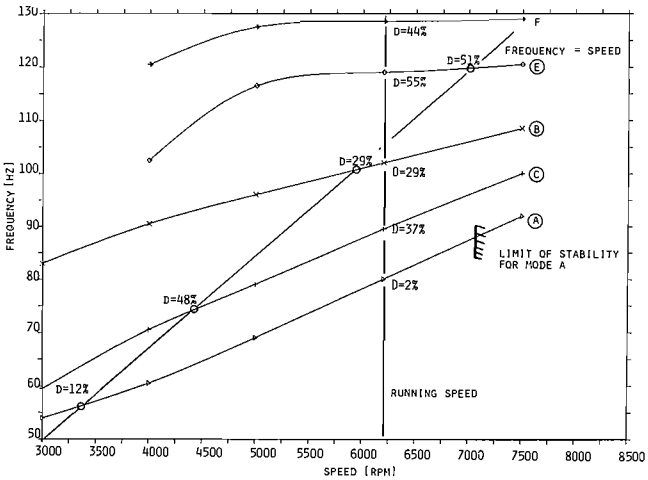

Figure 7. Campbell Diagram, Case 4.

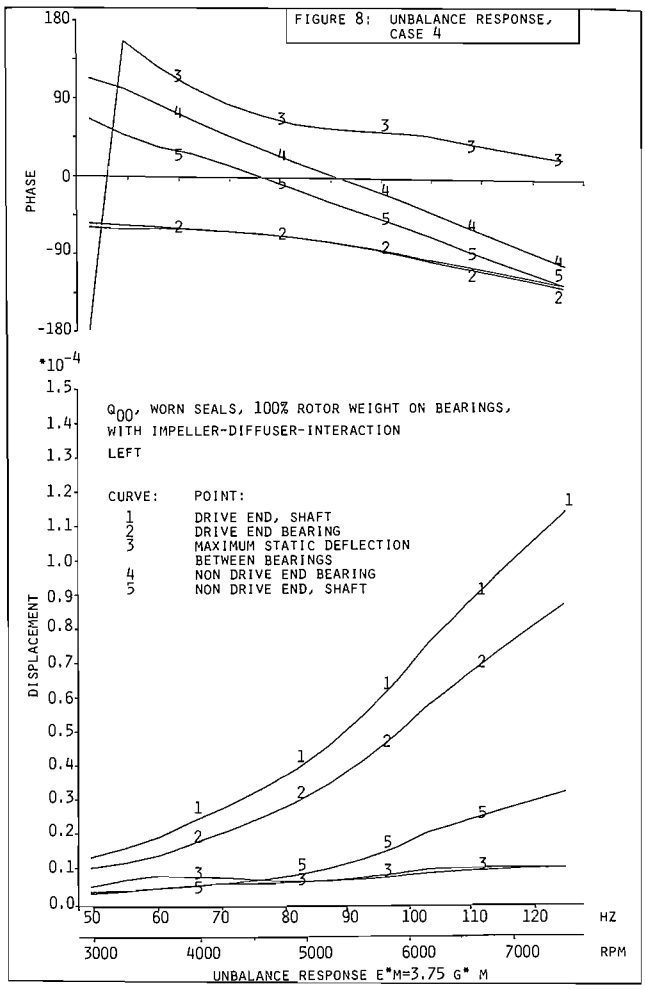

Figure 8. Unbalance Response, Case 4.

The response to unbalance for Case 4 is shown in Figure 8. A slight resonant peak occurs for location 3 only, at 3500 cpm. This corresponds to the intersection of the running speed with the eigenfrequency for mode shape "A" in Figure 7, at a damping value of 12 percent. This is the lowest, damped "critical speed." Intersections with mode "C", "B" and "E" at 4500 cpm, 6000 cpm and 7200 cpm produce no noticeable response—all these modes are too heavily damped. Even for the case of a "critical speed" close to running speed, there is no danger of a resonant amplitude increase in the pump.

Returning to the general overview of the results, a graphic illustration (Figure 9) shows what happens to the least damped eigenfrequency when parameters are changed one at a time:

- Cases 1 and 2 have the highest eigenfrequencies, because of the new seal clearances which give higher direct stiffness than with the worn clearances. These cases also have the highest damping, except for the cases with swirl breaks, Cases 7 and 8.
- When impeller forces are introduced into the model, eigenfrequencies decrease: Case 1 to 2 for new clearances and Case 3 to 4 for worn clearances. The addition of impeller forces always decreased damping.
- The wear of the seals, Case 2 to 4 with impeller forces and Case 1 to 3 without impeller forces, has the most significant negative effect of all parameters considered. Both eigenfrequency and damping decrease dramatically.
- When the bearing load decreases as a result of static radial thrust, the eigenfrequency decreases and the damping remains almost constant: Case 4 to 5.

Cases 4 and 5 show good agreement with the measured results. The actual bearing load must be somewhere between what has been assumed for Cases 4 and 5. Measurement showed a vibrational peak starting to rise at approximately 0.73 × (running speed), Figure 10. The rotor is not yet unstable, but the limit of stability is almost reached, i.e., damping is almost zero. The calculated damping for Cases 4 and 5 is still a little high. As indicated in Figure 7, the calculated instability would be reached at 7100 cpm, whereas measurements lead to the conclusion that the pump with worn seal clearances would become unstable at about 6500 cpm. In determining whether a pump will perform reliably or not, this speed, for the onset of instability, is the most important criterion, not "critical speeds." In a well designed pump, "critical speeds" are normally too heavily damped, even in the worn condition, to be excited.

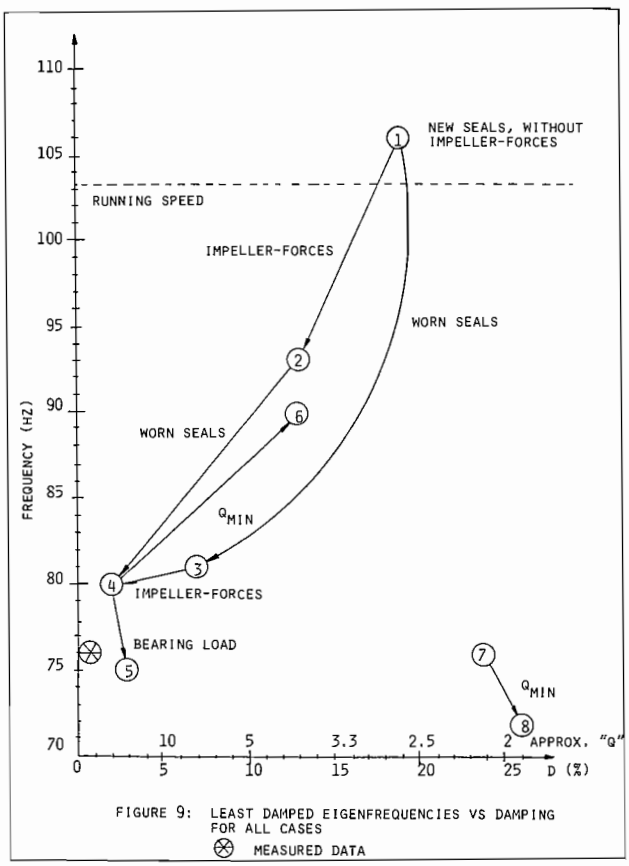

Figure 9. Least Damped Eigenfrequencies vs. Damping For All Cases.

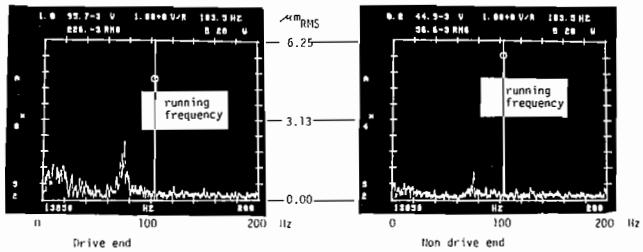

Figure 10. Measured Vibrations at BEP, Worn Seals.

At minimum flow, eigenfrequency and damping increase so much that there is no danger of rotordynamic instability, even with worn clearances, Case 4 to 6. This results from the higher pressure difference across the seals and lower tangential velocities in front of them. No subsynchronous resonant peak was measured at minimum flow.

By comparing Cases 6 and 8, and Cases 4 and 7, it can be seen that swirl breaks reduce the eigenfrequency dramatically; the direct stiffness and cross-coupled damping is lower for all seals and impellers. The big advantage is the very significant reduction in the coefficient K_{12}, the cross-coupled stiffness, which reduces the forward driving tangential force. Overall damping is also increased because of this effect. The model with the swirl breaks has higher damping with worn seals than the one without swirl breaks has with seals! There is no possibility for instability to occur. However, tests on the machine for [16] have shown that swirl breaks influence axial thrust and leakage flow.

For the purpose of developing a better understanding of the results, Figures 11, 12, and 13 were created based on the following simplifying assumptions:

- The shaft motion can be described as a forward whirling circular orbit, such that the tangential force in the direction of rotation can be expressed as [16]:

$$F_t^* = K_{12}^* - C_{11}^*\left(\frac{\Omega}{\omega}\right) - m_{12}^*\left(\frac{\Omega}{\omega}\right)^2 \qquad (7)$$

where the coefficients are normalized according to Equations (2), (3) and (4) and ω is the running frequency and Ω is the whirl frequency.

- The influence of the mode shape is small, i.e., the radii of orbit at each location along the shaft are the same.
- The influence of the journal bearings is small, i.e., bearings are located near nodes so that displacement is nearly zero.

With these assumptions and Figures 11, 12 and 13, it can be seen that the forward and backward tangential force components at the impellers and balance piston are several times larger than those at the seals. The fact that the resultant driving force is

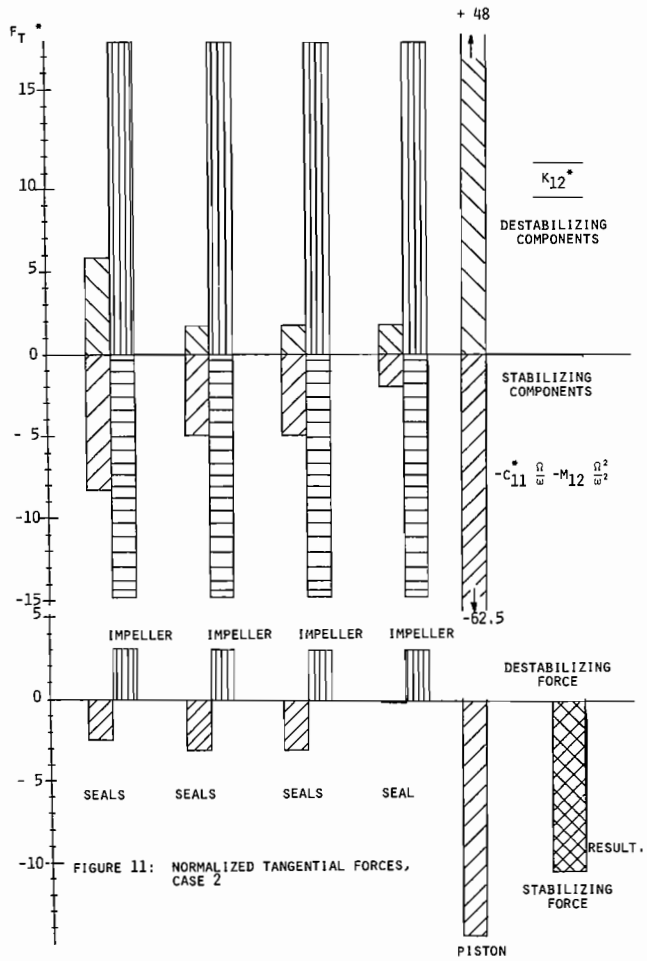

FIGURE 11: NORMALIZED TANGENTIAL FORCES, CASE 2

Figure 11. Normalized Tangential Forces, Case 2.

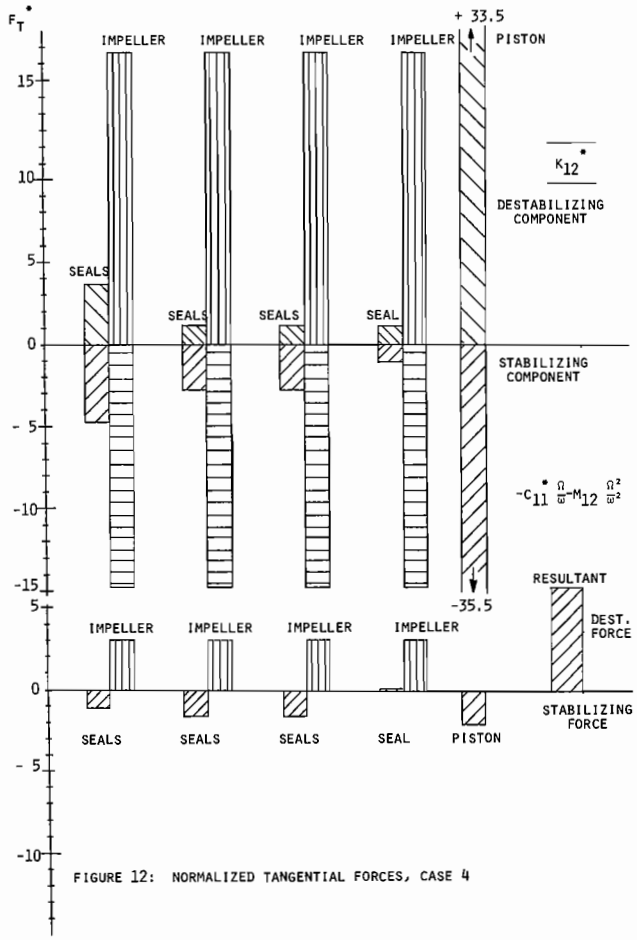

FIGURE 12: NORMALIZED TANGENTIAL FORCES, CASE 4

Figure 12. Normalized Tangential Forces, Case 4.

the difference of two large values produces uncertainties. Small relative errors in one of the two components leads to very large errors in this difference. The resultant force for the impellers is slightly larger than the resultant for the new seals (Figure 11). However, the balance piston, with new clearances, produces such a large driving backward tangential force that the net resultant becomes stabilizing. With worn seals, (Figure 12) the resultant forces for the impellers remain the same, but the resultant for the seals are reduced to about half and the piston forces are reduced significantly. The overall resultant for the impellers, seals and piston becomes forward driving and is destabilizing. Introducing swirl brakes (Figure 13) produces forces at the worn seals and the balance piston of approximately the same values as for new clearances. An even more striking effect is the change the impeller forces. The resultant tangential force at the impeller is changed from destabilizing to stabilizing. A forward driving force no longer exists at any location and the resultant stabilizing effect becomes the largest.

A comparison with Figure 9 indicates that the relative changes in damping predicted by these simplified calculations agree with the detailed analysis. The mode shape, and in particular bearings, were not taken into account and, therefore, the absolute value of damping is not correct. The negative resultant for Case 4, (Figure 12) indicates that the pump is already unstable, which is not true, neither by detailed calculation nor by measurement. However, these hand calculations can be a valuable tool in predicting potential problems for a pump without resorting to extensive detailed analysis.

CONCLUSIONS

The research results show that impeller forces must be included in the rotordynamic models of high energy, multistage pumps. The forces tend to lower the natural frequencies and reduce damping. Based on the best presently available rotordynamic coefficients, good agreement was achieved, for a boiler feed pump with enlarged clearances, operating near its stability limit, for both natural frequency and damping. The only model adaptation necessary was the reduction of the direct stiffness term for the impeller forces.

The pump investigated has a relatively large diameter shaft and short bearing span. For this pump, the addition of impeller forces to the model resulted in the prediction of a "critical speed" below the operating speed, even with new seal clearances. With two times the new clearances, three "critical speeds" were predicted below the operating speed. High speed multistage pumps will generally have natural frequencies below the running speed; this will certainly be the situation for enlarged seal clearances. However, if damping is sufficient, the response when running through or even at these natural frequencies will be low, as has been demonstrated in this paper. The analysis points out that rotor response and stability limits are the key factors which limit the reliability of multistage pumps. This is contrary to the approach which is currently taken in many specifications which require these multistage pumps to run subcritically, i.e., below the first rotor natural frequency. Better criteria must be found for defining good rotordynamic

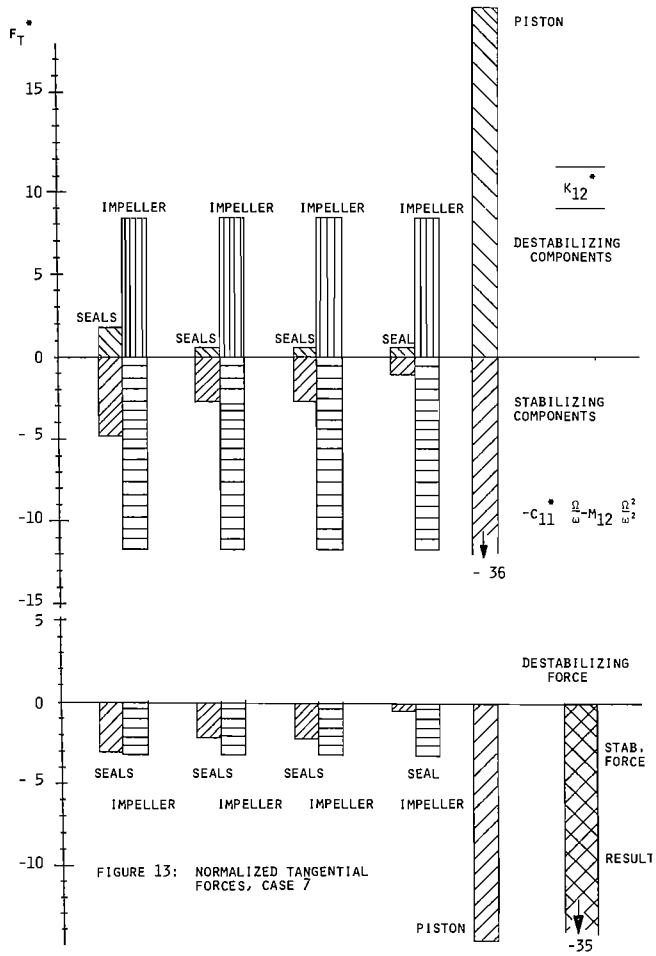

FIGURE 13: NORMALIZED TANGENTIAL FORCES, CASE 7

Figure 13. Normalized Tangential Forces, Case 7.

behavior; these new criteria should be based on the response of the rotor to external forces such as unbalance.

In Figures 11, 12 and 13, it was shown that the net damping is the difference between large forces, and is, therefore, very sensitive to changes in these forces. This explains why, with increased clearances, especially at the balancing piston, the damping of the rotor decreases significantly. On the other hand, it highlights the fact that relatively small modifications, such as swirl breaks, reducing the cross-coupled stiffness terms, can provide the opportunity to make dramatic increases in rotor stability. It also helps explain the frequently observed situation where supposedly identical pumps exhibit very different vibration behavior.

Although the addition of impeller forces has improved the rotordynamic model, more work is needed in the following areas:

- Experimental verification of rotordynamic coefficients for seals and impellers at speeds and temperatures typical of boiler feed pumps.
- Investigation of secondary effects of swirl breaks, e.g., axial thrust and efficiency.
- Indications are that the forces acting on the impeller shroud may be just as large or larger than the hydraulic forces originating in the impeller channels. Impeller shroud geometry may therefore be important, and the measurements of impeller forces without representative shroud geometries may be misleading.
- Theoretical studies, yielding impeller force coefficients, for the shroud forces and the forces from the impeller channels, should be pursued, to supplement experimental data.

Work on the first three points is part of the ongoing EPRI project [15]. The test rig for the measurement of impeller forces [16] will be operated at 4000 cpm and up to 180°C during 1986 and subsequently modified for the measurement of seal coefficients at temperatures and speeds corresponding to boiler feed pump service.

REFERENCES

1. Makay, E., "How Close Are Your Feed Pumps to Instability-Caused Disaster?," Power (December 1980).
2. Bolleter, U., Frei, A., and Florjancic, D., "Predicting and Improving the Dynamic Behavior of Multistage High Performance Pumps," *Proceedings of the 1st International Pump Symposium*, Turbomachinery Laboratories, Department of Mechanical Engineering, Texas A&M University, College Station, Texas (1984).
3. American Petroleum Institute, "Centrifugal Compressors for General Refinery Services", *API Standard 617*.
4. Orcutt, F. K., "The Steady State and Dynamic Characteristics of a Full Circular Bearing and a Partial Arc Bearing in the Laminar and Turbulent Flow Regimes," Journal of Lubricating Technology, (April 1967).
5. Schaffrath G., "Ein Verfahren zum Berechnen der vier Feder- und vier Dämpfungskoeffizienten von Radialgleitlagern Forschung und Ingenieurwesen," *6* (1969).
6. Glienicke J., "Esperimentelle Ermittlung der Statischen und Dynamischen Eigenschaften von Gleitlagern für Schnellaufende Wellen," Fortschrittsberichte VDI-Z Reihe 1, *22* (1970).
7. Lund, J. E. and Thompson, K. K., "A Calculation Method and Data for the Dynamic Coefficients of Oil-lubricated Journal Bearings: Topics in Fluid Film Bearing and Rotor Bearing System Design and Optimization," ASME, p. 1 (1978).
8. Black, H. F., "Effects of High Pressure Ring Seals on Pump Rotor Vibration," ASME, (1971).
9. Black, H. F., "Inlet Flow Swirl in Short Turbulent Annular Seal Dynamics," 9th International Conference of Fluid Sealing (April 1981).
10. Childs, D. W., "Dynamic Analysis of Turbulent Annular Seals, Based on Hirs' Lubrication Equation," ASME 82-Lub-41 (1982).
11. Childs, D. W., "Finite Length Solution for Rotordynamic Coefficients of Turbulent Annular Seals," ASME 82-Lub-42 (1982).
12. Hergt, P., and Krieger, P., "Radial Forces in Centrifugal Pumps with Guide Vanes," Proc. Institute of Mechanical Engineering 184 (1969-1970).
13. Chamieh, D.S., et al., "Experimental Measurements of Hydrodynamic Stiffness Matrices for a Centrifugal Pump Impeller," NASA Conference Publication 2250 (1982).
14. Jery, B., Acosta, A. J., Brennen, C. E., and Caughey, T. H., "Hydrodynamic Impeller Stiffness, Damping and Inertia in the Rotordynamics of Centrifugal Flow Pumps," Third Workshop on Rotor Instability Problems in High Performance Turbomachinery, Texas A&M University, College Station, Texas (May 1984).

15. Sulzer/EPRI contract RP 1884-10, "Feed Pump Hydraulic Performance and Design Improvement," (May 1983).

16. Bolleter, U., and Wyss, A., "Measurement of Hydrodynamic Interaction Matrices of Boiler Feed Pump Impellers," ASME 85-DET-148 (1985).

17. Madyn, Ing. Büro Kelment, Alkmaarstr. 37, 6100 Darmstadt 13, W. Germany (September 1984).

18. Nohring, U.K., "Untersuchung des radialen Druckverlaufes und des ubertragenen Drehmomentes im Radseitenraum von Kreiselpumpen bei glatter, ebener Radseiten wand und bei Anwendung von Ruckenschaufeln," Dissertation, Technische Universitat Braunschweig (1976).

19. Massey, I., "Subsynchronous Vibration Problems in High Speed Multistage Centrifugal Pumps," *Proceedings of the 14th Turbomachinery Symposium*, Turbomachinery Laboratories, Department of Mechanical Engineering, Texas A&M University, College Station, Texas (1985).

20. Nordmann, R. and Massmann, H., "Identification of Dynamic Coefficients of Annular Turbulant Seals," pp. 295-311, NASA Conference Publication 2338, Proceedings of Rotordynamic Instability Problems in High Performance Turbomachinery and Workshop, Texas A&M University (1984).

21. Ohashi, H. and Shoji, H., "Lateral Fluid Forces Acting on a Whirling Centrifugal Impeller in Vaneless and Vaned Diffuser," Proceedings of Rotordynamic Instability Problems in High Performance Turbomachinery Workshop, Texas A&M University, p. 109-122 and NASA Conference Publication 2338.

22. Brennen, C., "On the Flow in an Annulus Surrounding a Whirling Cylinder," *Journal of Fluid Mechanics*, 75, (1), pp. 173-191 (1976).

ACKNOWLEDGEMENTS

Members of the Project Advisory Panel for EPRI research project RP1884-10, Feed Pump Hydraulic Performance and Design Improvement.